Application of the Finite-Momentum Pairing Method 1

?? introduced the method of enforcing a finite momentum on the order parameter to gain access to the coherence length ξ_0 and the London penetration depth $\lambda_{L,0}$.

In this chapter, it will be applied in two ways. In section 1.1 for the decorated graphene model on the mean-field level. Here, the influence of the quantum geometry on superconductivity as explained in **??** will be explored.

In section 1.2, it is then applied to the one-band attractive Hubbard model on the square lattice, both on the mean-field level and using Dynamical Mean Field Theory (DMFT). It has one parameter tuning the attractive interaction between electrons, making it the prime example for demonstrating the BCS-BEC crossover phenomenon in the DMFT implementation.

1.1 Decorated Graphene Model

By self-consistently solving the gap equation **??** for a set of external parameters, the behavior of the gap values Δ_α for the three orbitals $\alpha \in \{\mathrm{Gr_A}, \mathrm{Gr_B}, \mathrm{X}\}$ can be analyzed. In the case of the decorated graphene model, these are the Hubbard interaction U (here set the same for all orbitals), the hybridization V, temperature T and Cooper pair momentum $\mathbf{q}$. All steps are shown for an example value of $U = 0.1t$, results for the superconducting length scales will later be compared between different U.

Critical Temperatures

The zero-temperature lengths $\xi_0, \lambda_{L,0}$ are extracted from the temperature dependence $\xi(T), \lambda_L(T)$ in **??** and **??** (which both depend on the ration T/T_C). This means the first step in the analysis is to find the critical temperature T_C for $\mathbf{q} = 0$.

Because the calculations near T_C are hard to converge, finding T_C by analyzing the point at which the gap vanishes is not feasible. Instead, from the Ginzburg-Landau theory expression **??** (which is valid for $T \simeq T_C$), the T_C can be extracted from the linear behavior of the order parameter near the phase transition:

$$|\Delta_\alpha|^2 \propto T_C - T \, . \tag{1.1}$$

This is shown in fig. 1.1. Notable here is that even though Δ_A is orders of magnitude smaller than Δ_B and Δ_X, T_C is the same for every orbital. This is the case for all values

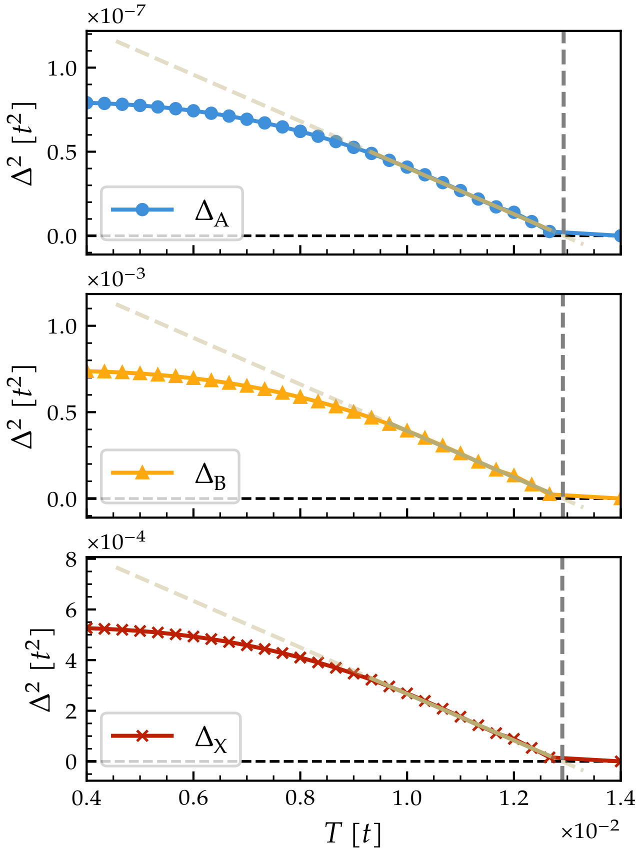

Figure 1.1 – Extraction of T_C from the linear behavior of the order parameter. Shown is the square of the gap Δ_α near T_C for $U = 0.1t$, $V = 1.6t$ and $\mathbf{q} = 0$. The linear fit for extracting T_C is shown in tan, the corresponding T_C is marked by the dashed gray line.

of V, as shown in fig. 1.2a. Figure 1.2b shows that T_C follows the maximal value of the Δ_α, switching over from X to $\mathrm{Gr_B}$ at $V = 1.46t$.

The value of Δ_α follows the corresponding orbital weight $w_\alpha, \alpha \in \{\mathrm{Gr_A}, \mathrm{Gr_B}, \mathrm{X}\}$ of the flat band as shown in **??**. In contrast to a repulsive Hubbard interaction [1] there is no gap closure for a medium V, there is just a minimum of the maximal gap value at $V = 1.46t$.

Extracting the Superconducting Length Scales

The correlation length $\xi(T)$ is associated with the breakdown of the order parameter:

$$|\Psi_{\mathbf{q}}|^2 = |\Psi_0|^2 \left(1 - \xi(T)^2 q^2\right) , \tag{1.2}$$

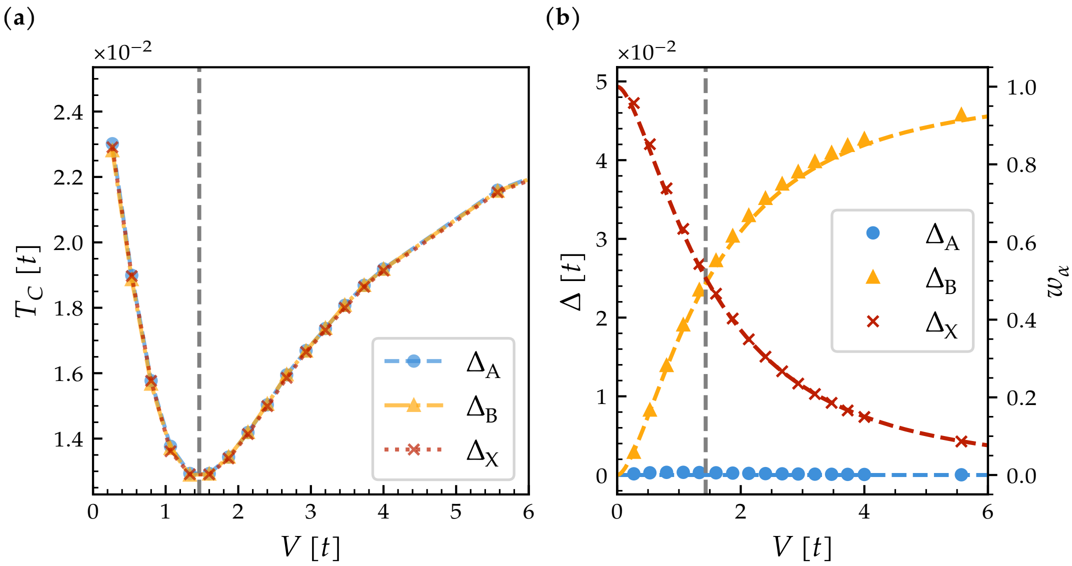

Figure 1.2 – Critical temperatures and gaps against V**.** (**a**) T_C against hybridization V, the same for all three orbitals. (**b**) Gaps Δ_α for the same values of V. The dashed lines are the orbital weight of the flat band as defined in **??**. The dashed value $V = 1.46t$ is taken from the minimum of $T_C(V)$, coinciding with the switchover of the orbital character. Both plots are for the same $U = 0.1t$ and $\mathbf{q} = 0$.

which means that the q_C where the order parameter breaks down is related to the correlation length via

$$\xi = \frac{1}{q_C} . \tag{1.3}$$

The momentum $\mathbf{q}$ is chosen as $\mathbf{q} = q \cdot \mathbf{b}_1$ with the reciprocal vector $\mathbf{b}_1$ and $q \in [0, 0.5]$. For $q > 0.5$, the vector is outside of the first Brillouin zone and the behavior of $\Delta_\alpha(\mathbf{q})$ is periodic from that point. This means the maximal ξ that can be resolved in this method is given by

$$\xi = \frac{1}{0.5 \cdot |\mathbf{b}_1|} = \frac{\sqrt{3}a}{2\pi} = \frac{3a_0}{2\pi} . \tag{1.4}$$

Similar to finding T_C, numerical calculations near q_C are hard to converge, so instead the criterion employed here is to choose $\mathbf{Q}$ such that

$$\left| \frac{\psi_{\mathbf{Q}}(T)}{\psi_0(T)} \right| = \frac{1}{\sqrt{2}} , \tag{1.5}$$

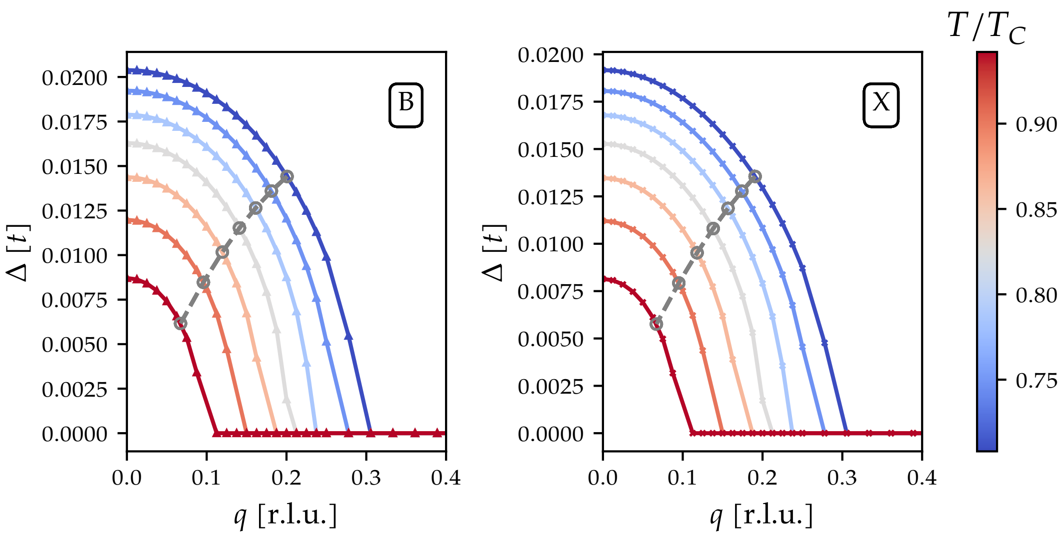

Figure 1.3 – Suppression of the order parameter with q for $V = 1.5t$ **and** $U = 0.1t$**.** The x-axis is marked in relative lattice units, i.e. $\mathbf{q} = q \cdot \mathbf{b}_1$ for the reciprocal unit vector $\mathbf{b}_1$. Marked in gray are the points at which the gaps have fallen off to $1/\sqrt{2}$ of their value at $\mathbf{q} = 0$.

and then take

$$\xi = \frac{1}{\sqrt{2}|\mathbf{Q}|} . \tag{1.6}$$

This is not the only way to extract information from the **q**-dependence of the order parameter, compare ref. [2] for discussion about this method and comparison to other methods.

As shown in fig. 1.2b, only Δ_B and Δ_X have a significant magnitude in the parameter range of U considered here. So for these two, the **q**-dependence is shown in fig. 1.3. Chosen here is $V = 1.5t$, so in the parameter regime switching over between dominating X and B contribution. Both gaps have a q_C for which the gap vanishes as shown in **??**. For higher temperatures q_C goes to 0, showing how the correlation length diverges for $T \to T_C$.

In the case of high and low V, the superconducting order is dominated by one of Δ_A, Δ_X. Figure 1.4 shows that the gap does not fully go down to 0 for $\mathbf{q} = 1/2 \cdot \mathbf{b}_1$, meaning that in these cases the correlation length calculated in Ginzburg-Landau theory is smaller than $3a_0/2\pi$.

The Ginzburg-Landau free energy is an quadratic expansion in the order parameter and thus only applicable near T_C and for low **q**. Figure 1.4 shows cases where this is not the case and the picture in fig. 1.2b does not hold true. It is still possible to extract

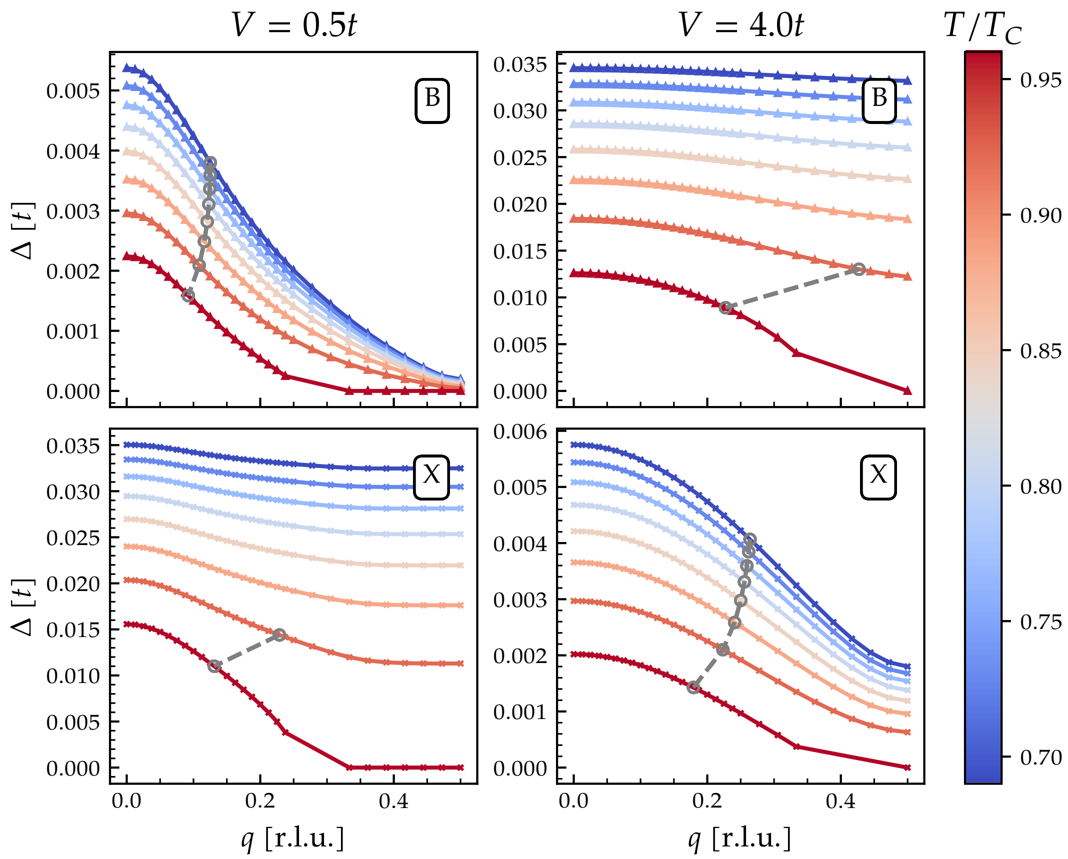

Figure 1.4 – Suppression of the order parameter with q for $V = 0.5t$ and $V = 4t$ (both for $U = 0.1t$). In contrast to fig. 1.3, in this parameter regime the order parameter is fully suppressed for the maximal $q = 0.5$.

values for $|\mathbf{Q}|$ especially for $T \to T_C$, but it should be kept in mind that in the low and high V limit, the analysis loses its foundation.

To calculate the London penetration depth λ_L via

$$\lambda_L(T) = \sqrt{\frac{\Phi_0}{3\sqrt{3}\pi\mu_0\xi(T)j_{dp}(T)}}, \tag{1.7}$$

also the depairing current j_{dp}, the maximum of the superconducting current $\mathbf{j}(\mathbf{q})$ is needed. Figure 1.5 shows the current $j(\mathbf{q}) = |\mathbf{j}(\mathbf{q})|$ with the maximum marked for every temperature. Similar to the gaps, the current shows the behavior sketched in **??** for $V = 1.5t$, but for the low and high V values, the current is not fully suppressed for the lower temperatures and at $q = 0.5$. Still, a maximum can be extracted, but a similar

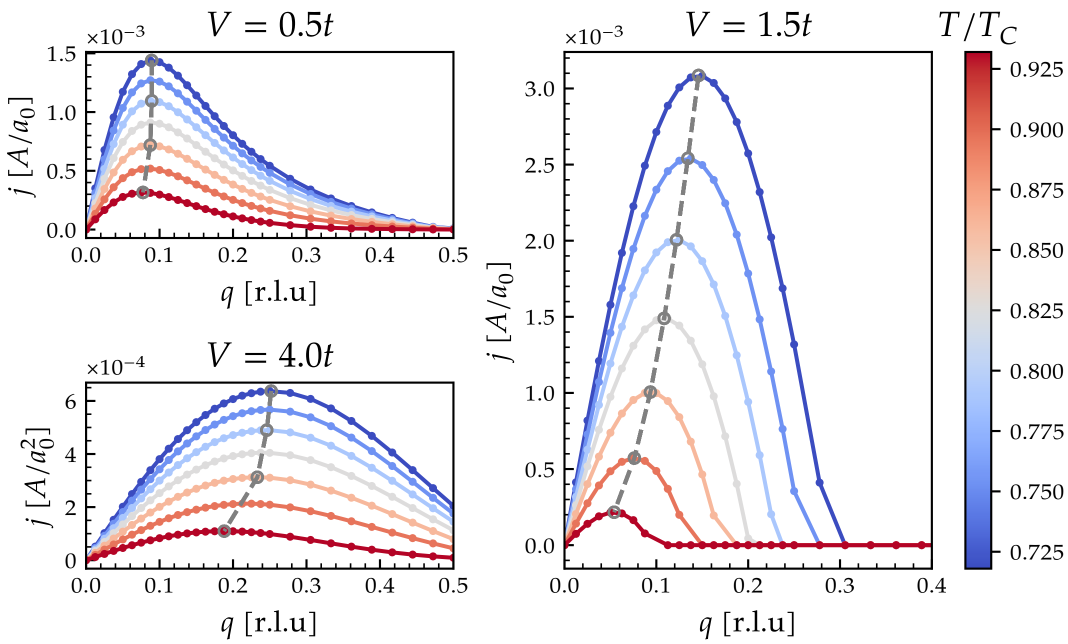

Figure 1.5 – Superconducting current from a finite q for $U = 0.1t$. For calculation of the London penetration depth λ_L, the maximum j_{dp} of the current is needed, marked here in gray .

caveat as in the discussion of the gaps about the applicability of the Ginzburg-Landau expressions applies.

Figure 1.6 shows the temperature dependence for $\xi(T)$ and $\lambda_L(T)$ for $V = 1.5t$. These can be fit to the Ginzburg-Landau expressions

$$\xi(T) = \xi_0 \left(1 - \frac{T}{T_C}\right)^{-\frac{1}{2}} \tag{1.8}$$

and

$$\lambda_L(T) = \lambda_{L,0} \left(1 - \frac{T}{T_C}\right)^{-\frac{1}{2}} \tag{1.9}$$

to obtain the zero-temperature values ξ_0 and $\lambda_{L,0}$.

Length Scales

Figure 1.7 shows the extracted length scales for two different values of the attractive interaction U. For the coherence length, the behavior is similar between the two

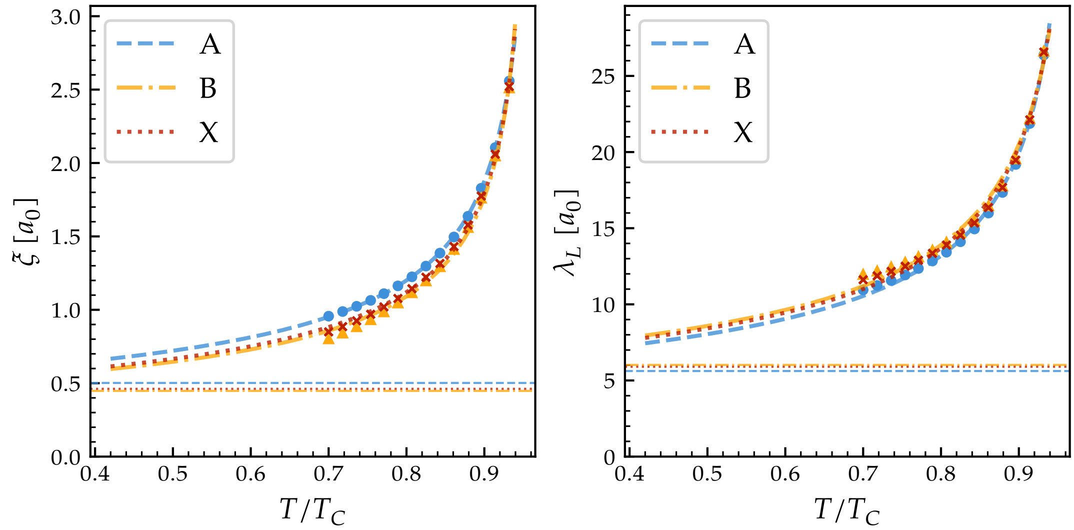

Figure 1.6 – Temperature dependence of the correlation length ξ and London penetration depth λ_L for $V = 1.50t$ and $U = 0.1t$. The fits for extracting the zero-temperature values ξ_0, $\lambda_{\mathrm{L},0}$ and the corresponding values are marked as dashed lines.

values: the orbital with the largest gap value has the shortest coherence length, with a switchover between the small and large V values at around $V = 1.46t$, the point at which the dominating gap switches over from the X to the B orbital. Between **??** and **??**, the larger attractive interaction leads to a smaller coherence length around $V = 1.46t$. Interestingly, the orbitals with vanishing gap in the large V-limit go to the same value of ξ_0, independent of U. The London penetration depth has a minimum around the switchover point $V = 1.46t$ that is smaller with larger U. This shows that the superfluid weight

$$D_\mathrm{S} \propto \lambda_{\mathrm{L},0}^{-2} \tag{1.10}$$

is suppressed for large values of V.

Another way to calculate the superfluid weight from linear response theory was introduced in **??**. Figure 1.8 shows the superfluid weight from the $\mathbf{q}$-dependence and the linear response formula, specifically $D_{\mathrm{S},xx} + D_{\mathrm{S},yy}$. This is be split up between the geometric and the conventional contribution. Also shown is the minimal quadratic Wannier spread

$$\Omega_\mathrm{I} = \mathrm{Tr}\, M_{\mu\nu} = \frac{1}{N_\mathbf{k}} \sum_\mathbf{k} g_{xx}(\mathbf{k}) + g_{yy}(\mathbf{k}) \tag{1.11}$$

calculated from the quantum metric $g_{\mu\nu}(\mathbf{k})$. It shows that the condition under which the superfluid weight is entirely determined by the geometric contribution [3] occurs in the case of an isolated flat band: for U smaller than the gap separating the flat band

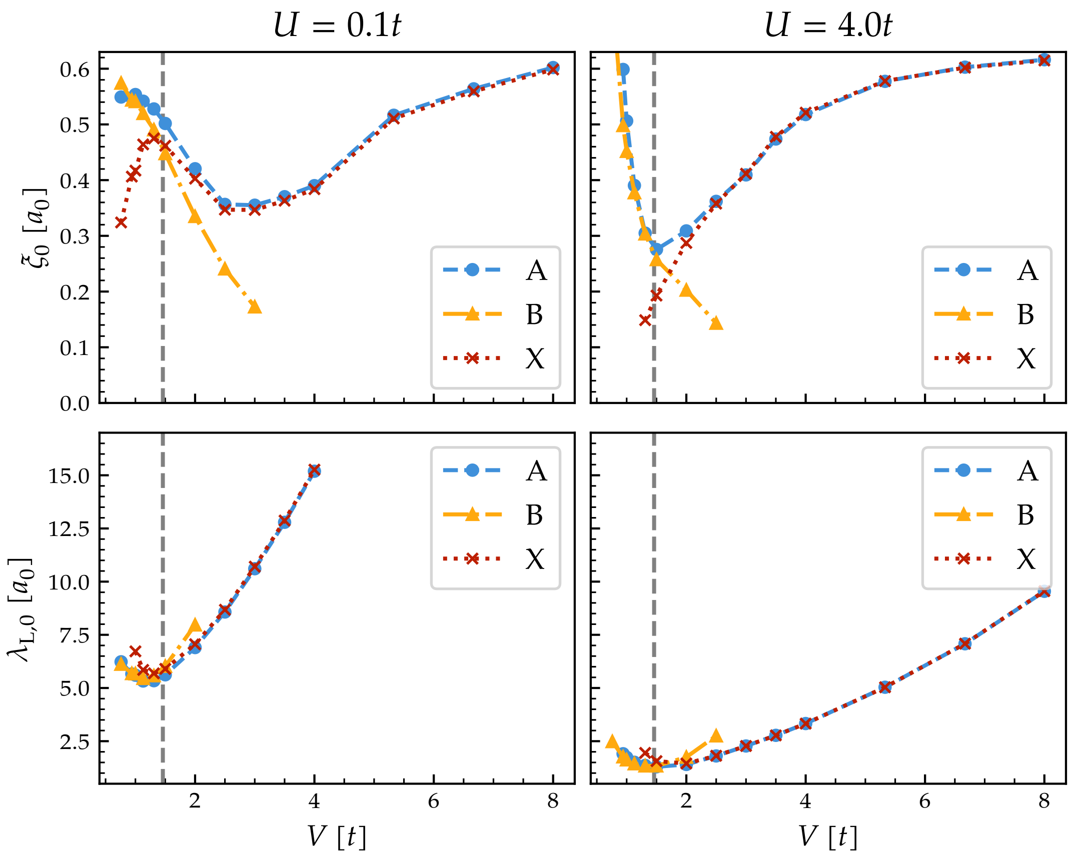

Figure 1.7 – Superconducting length scales for $U = 0.1t$ **and** $U = 4.0t$**.** Marked in gray is $V = 1.46t$, the point at which the dominating gap switches over from the X to the B orbital.

from the dispersive bands (which is $\mathcal{O}(V)$, this condition holds. However, for instance, when $U = 1.0t$, the conventional contribution increases, and for $U = 6.0t$, it becomes dominant until $U \sim V$.

The results from the Finite Momentum Pairing (FMP) method agree with the linear response insofar that they show a peak in the intermediate V-regime and go to zero for $V \to 0$ and $V \to \infty$, but the location of this peak is not the same between the two methods.

The critical temperatures in BCS theory as seen in fig. 1.2a shows a minimum in the intermediate V region, while the superfluid weight has its maximum in this region. In consequence, because a finite superfluid weight is needed to support superconductivity, the analysis from BCS theory suggests that the optimum for superconductivity is in this region and not for $V \to 0$ or $V \to \infty$ where T_C is largest.

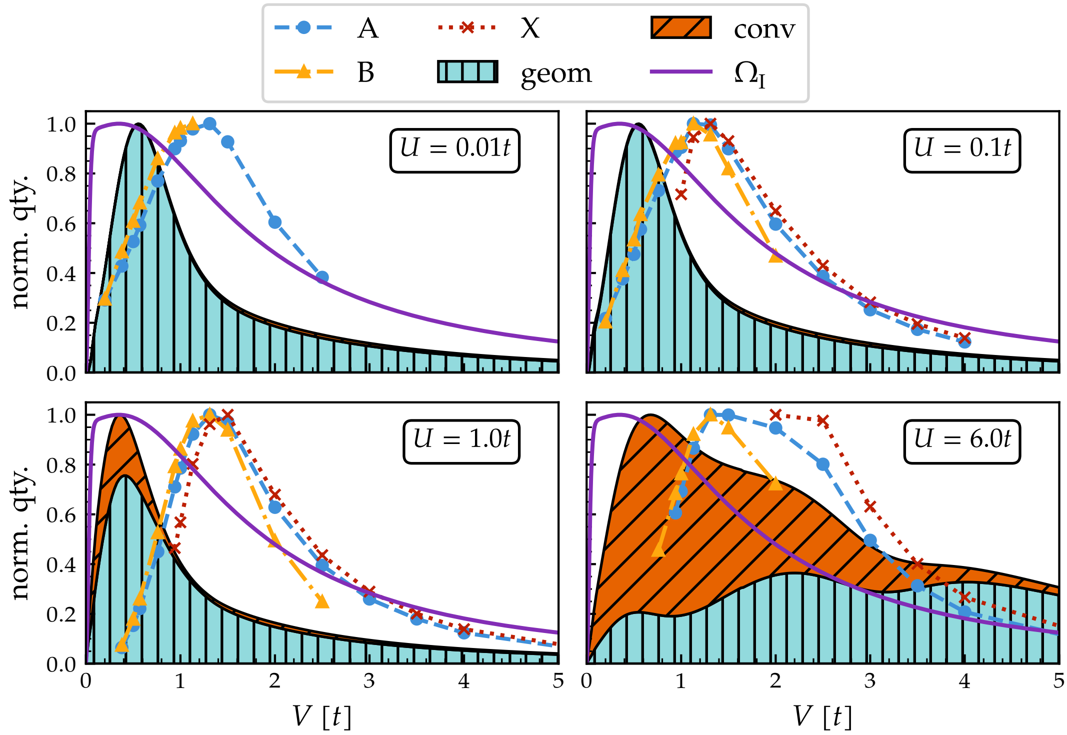

Figure 1.8 – Comparison of the superfluid weight calculated by different methods. All quantities are normalized to analyze the general trend in comparison to the minimal quadratic Wannier spread Ω_I. For the calculation coming from linear response theory (see **??**), the geometric and conventional contributions are marked separately.

1.2 One-Band Hubbard Model

DMFT gives insight into the phenomenon of the BCS-BEC crossover [4–7]. To study this, the FMP method is applied for a simpler model in the Hubbard model on the square lattice with only one orbital per unit cell. T_C can be extracted from the linear behavior of Δ^2 the same way as above, fig. 1.9a shows T_C against U calculated in both BCS and DMFT. This shows how the BCS T_C only describes the pairing temperature and in DMFT, also phase coherence is captured. The DMFT curve shows the typical dome-shape of the BCS-BEC crossover with stronger attractive interaction.

The extraction of the superconducting length scales works the same as in section 1.1. Figure 1.9b shows how these length scales characterize the BCS-BEC crossover phenomenon: the coherence length goes to a constant value when going into the BEC regime, marking how the Cooper pairs become strongly localized. For $U \sim 1.0t$ the DMFT calculations were difficult to converge, so especially the values for $\lambda_{L,0}$ vary in

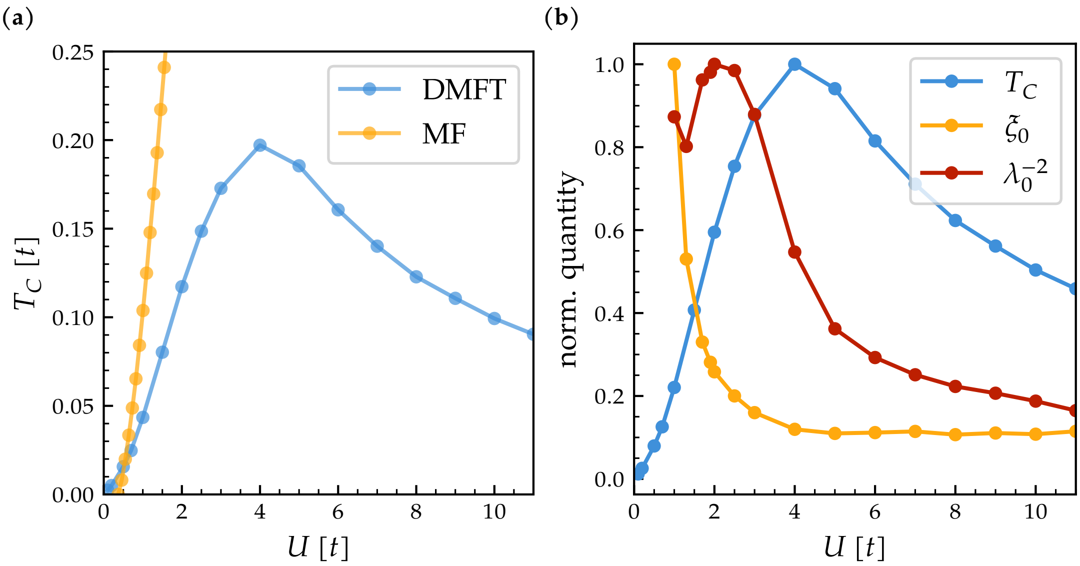

Figure 1.9 – T_C and superconducting length scales for the one-band Hubbard model. (**a**) T_C calculated from mean-field theory and DMFT respectively. It shows the characteristic dome of the BCS-BEC crossover that is not captured in mean-field theory. (**b**) Critical temperature T_C, coherence length ξ_0 and superfluid weight $D_\mathrm{S} \propto \lambda_{\mathrm{L},0}^{-2}$ normalized to its maximal value. In the crossover to the BEC-regime, the superfluid weight goes to 0 and the coherence length goes to a constant value.

this regime, but regardless the superfluid weight has its maximal value for low U and goes to zero for stronger attractive interaction.